J. Mol. Biol. (1994) 236, 800–816

Crystal Structure of *Escherichia coli* Thioredoxin Reductase Refined at 2 Å Resolution

Implications for a Large Conformational Change during Catalysis

Gabriel Waksman[1]†‡, Talluru S. R. Krishna[1,2]†, Charles H. Williams Jr[3] and John Kuriyan[1,2]§

[1]*Laboratories of Molecular Biophysics and* [2]*Howard Hughes Medical Institute The Rockefeller University, 1230 York Avenue, New York, NY 10021, U.S.A.*

[3]*Department of Veterans Affairs Medical Center and Department of Biological Chemistry The University of Michigan, Ann Arbor, MI 48105, U.S.A.*

The crystal structures of three forms of *Escherichia coli* thioredoxin reductase have been refined: the oxidized form of the wild-type enzyme at 2·1 Å resolution, a variant containing a cysteine to serine mutation at the active site (Cys138Ser) at 2·0 Å resolution, and a complex of this variant with nicotinamide adenine dinucleotide phosphate ($NADP^+$) at 2·3 Å resolution. The enzyme mechanism involves the transfer of reducing equivalents from reduced nicotinamide adenine dinucleotide phosphate (NADPH) to a disulfide bond in the enzyme, *via* a flavin adenine dinucleotide (FAD). Thioredoxin reductase contains FAD and NADPH binding domains that are structurally similar to the corresponding domains of the related enzyme glutathione reductase. The relative orientation of these domains is, however, very different in the two enzymes: when the FAD domains of thioredoxin and glutathione reductases are superimposed, the NADPH domain of one is rotated by 66° with respect to the other. The observed binding mode of $NADP^+$ in thioredoxin reductase is non-productive in that the nicotinamide ring is more than 17 Å from the flavin ring system. While in glutathione reductase the redox active disulfide is located in the FAD domain, in thioredoxin reductase it is in the NADPH domain and is part of a four-residue sequence (Cys-Ala-Thr-Cys) that is close in structure to the corresponding region of thioredoxin (Cys-Gly-Pro-Cys), with a root-mean-square deviation of 0·22 Å for atoms in the disulfide bonded ring. There are no significant conformational differences between the structure of the wild-type enzyme and that of the Cys138Ser mutant, except that a disulfide bond is not present in the latter. The disulfide bond is positioned productively in this conformation of the enzyme, i.e. it stacks against the flavin ring system in a position that would facilitate its reduction by the flavin. However, the cysteine residues are relatively inaccessible for interaction with the substrate, thioredoxin. These results suggest that thioredoxin reductase must undergo conformational changes during enzyme catalysis. All three structures reported here are for the same conformation of the enzyme and no direct evidence is available as yet for such conformational changes. The simplest possibility is that the NADPH domain rotates between the conformation observed here and an orientation similar to that seen in glutathione reductase. This would alternately place the nicotinamide ring and the disulfide bond near the flavin ring, and expose the cysteine residues for reaction with thioredoxin in the hypothetical conformation. Such large-scale rotation is plausible because the NADPH domain of thioredoxin reductase makes relatively few inter-domain contacts with other parts of the dimeric enzyme. It is remarkable that these two enzymes, which catalyze very similar reactions and have clearly diverged from a common origin, are so different in the details of their active site architecture and their reaction mechanisms.

Keywords: thioredoxin reductase; glutathione reductase; conformational change; protein crystallography; disulfide oxidoreductase, flavin

† The first two authors contributed equally to this work.

‡ Present address: Departments of Biochemistry and Biophysics, Washington University School of Medicine, St Louis, MO, U.S.A.

§ Author to whom all correspondence should be addressed at Box 3, The Rockefeller University, 1230 York Avenue, New York, NY 10021, U.S.A.

0022-2836/94/080800-17 $08.00/0

1. Introduction

Thioredoxin reductase catalyzes the reduction by NADPH† of a redox-active disulfide bond in the small protein thioredoxin (Moore *et al.*, 1964; Zanetti & Williams, 1967; Ronchi & Williams, 1967; Thelander, 1968) and is a member of the family of pyridine nucleotide-disulfide oxidoreductases (Schirmer & Schultz, 1987; Williams *et al.*, 1991; Williams, 1992). These enzymes couple the oxidation of nicotinamide adenine dinucleotide (phosphate) (NAD(P)H) to the reduction of substrates, that usually contain disulfide bonds. The enzymes themselves contain a redox active disulfide and a tightly bound flavin cofactor (FAD). The flavin ring system mediates the transfer of reducing equivalents from NADPH to the disulfide bond. Other members of this enzyme family include glutathione reductase (Schulz *et al.*, 1978), mercuric ion reductase (Schiering *et al.*, 1991), lipoamide dehydrogenase (Mattevi *et al.*, 1991), trypanothione reductase (Kuriyan *et al.*, 1991*a*; Hunter *et al.*, 1992), NADH peroxidase (Stehle *et al.*, 1991, 1993).

Glutathione reductase is a well-understood member of this enzyme family, and it can serve as the prototype for describing the reaction mechanism. The availability of high resolution crystal structures for the enzyme alone and in complex with its substrates and cofactors has resulted in a detailed understanding of the structural basis of the reaction mechanism (Schulz *et al.*, 1978, 1982; Thieme *et al.*, 1981; Pai & Schulz, 1983; Karplus & Schulz, 1987, 1989; Pai *et al.*, 1988; Karplus *et al.*, 1989). The architecture of glutathione reductase is modular: there are two Rossman-type nucleotide-binding domains (Rossmann *et al.*, 1975) that bind FAD and NADPH, respectively. Figure 1 shows a schematic representation of the dimeric enzyme, based on Schulz *et al.* (1978) and illustrates how two sets of the nucleotide binding domains are brought together by a pair of "interface" domains. The binding site for NADPH places the nicotinamide ring in close contact with the *re* face of the flavin ring system, allowing the stereospecific transfer of a hydride ion (Manstein *et al.*, 1988). The enzyme's own disulfide bond, which is reduced by the flavin, is adjacent and on the other (*si*) side of the flavin ring system. This redox active disulfide bond is at the base of a deep crevice in the structure formed at the dimer interface in which glutathione binds. The

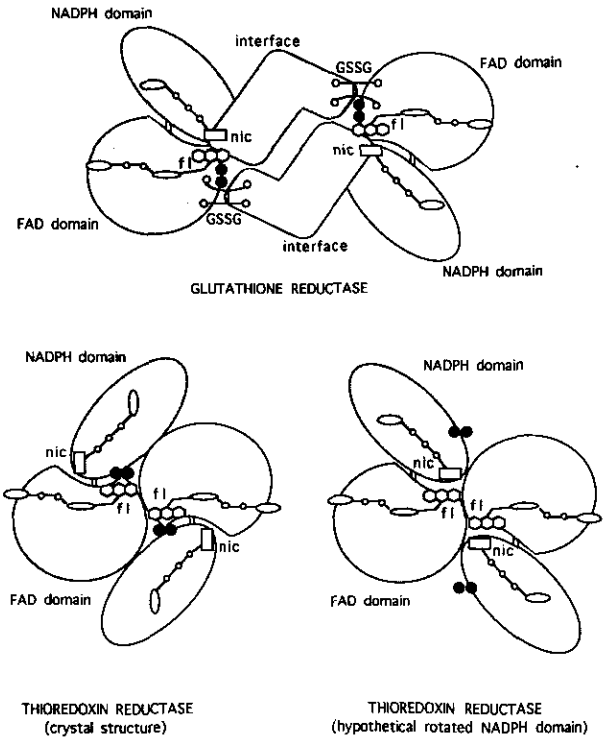

Figure 1. Schematic representation of the dimeric forms of glutathione reductase, thioredoxin reductase as derived from the crystal structure and thioredoxin reductase with a rotated NADPH domain (based on Schulz *et al.*, 1978). The rotation brings the NADPH domain into a configuration, with respect to the FAD domain, similar to that in glutathione reductase and also allows productive interaction between the nicotinamide ring of NAPDH and the isoalloxazine ring system of FAD. The isoalloxazine ring system, the nicotinamide ring and glutathione are indicated as fl, nic and GSSG, respectively. The enzyme's own disulfide group is indicated as 2 small black circles.

final step in the reaction, the disulfide/dithiol interchange with the substrate, occurs at this site. It is clear from the crystallographic studies that glutathione reductase has independent binding sites for all the players in the catalytic cycle. Thus, NADPH oxidation and substrate reduction can proceed with no major conformational changes in the enzyme. This enzyme architecture is seen to be essentially unchanged in mercuric ion reductase, trypanothione reductase, lipoamide dehydrogenase and NADH peroxidase.

In light of the fact that the prototypic glutathione reductase mechanism involves such exquisite spatial relationships between the different reaction partners, the gene sequence of thioredoxin reductase revealed surprising features (Russel & Model, 1988). On the one hand, sequence similarity with glutathione reductase indicated clearly that thioredoxin reductase is a closely related enzyme (Williams *et al.*, 1991). However, the interface domain of glutathione reductase is entirely missing. Since this domain is a central component of the dimer interface and the active site of glutathione reductase (see Fig. 1), thioredoxin reductase must have a com-

† Abbreviations used: NADPH, reduced nicotinamide adenine dinuclotide phosphate; FAD, flavin adenine dinucleotide; $NADP^+$, nicotinamide adenine dinucleotide phosphate; r.m.s., root-mean-square; F_o, observed structure factor; F_c calculated structure factor; α_c, calculated phase angle; $R_{symm} = \Sigma\Sigma(I_j - \langle I \rangle)/\langle I \rangle$, where I_j is a particular measured value of the intensity of a reflection, including symmetry related ones, and $\langle I \rangle$ is the average value of the intensity for that reflection. The inner summation is over all measurements for a particular reflection, and the outer summation is over all unique reflections.

Table 1
X-ray data collection and refinement statistics

	Resolution (Å)	Reflections	Unique	% Complete	R_{symm}†
A. *X-ray data collection*					
(Cys 138Ser) enzyme, FAST detector at Brookhaven Synchrotron	20·0 to 2·0	135,848	21,981	87	0·064
(Cys 138Ser) enzyme soaked with 10mM $NADP^+$, RAXIS on rotating anode	20·0 to 2·3	54,650	17,238	94	0·056
Wild-type enzyme, RAXIS in rotating anode	20·0 to 2·10	54,700	19,643	85	0·057

	(Cys138Ser) enzyme	(Cys138Ser) enzyme soaked in 10mM $NADP^+$	Wild-type enzyme
B. *Refinement*			
Resolution	6 to 2·0 Å	6 to 2·3 Å	6 to 2·1 Å
Reflections ($I > 2\sigma$)	21,102	16,181	18,508
Number of atoms	3494	3510	3494
Solvent molecules	164	158	164
Crystallographic *R*-factor	17·7%	17·9%	19·2%
r.m.s. deviation in bond length	0·017 Å	0·009 Å	0·008 Å
r.m.s. deviation in bond angles	2·9°	2·3°	2·3°

† R_{symm}, agreement factor between intensities of symmetry-related reflections.

pletely different architecture. Another surprising finding is that the enzyme's redox active disulfide is not present in the FAD domain (where it is found in glutathione reductase), but is, instead, in the NADPH domain. The crystal structure of a mutant thioredoxin reductase (Cys138Ser) has been determined previously (Kuriyan *et al.*, 1991*b*), and shows that the enzyme contains NADPH and FAD-binding domains that are very similar to those of glutathione reductase. Thioredoxin reductase is dimeric, but the dimer interface is formed mainly by the FAD domain instead of the interface domain, which is missing (Kuriyan *et al.*, 1991*b*). The NADPH domain is rotated by about 66° relative to its orientation in glutathione reductase. This results in the enzyme's redox active disulfide (located in this case in the NADPH domain) stacking against the *re* face of the flavin ring system in a position that corresponds to the location of the nicotinamide ring of NADPH in glutathione reductase. NADPH is known to transfer a hydride ion to the flavin with the same stereospecificity in thioredoxin reductase as is observed for glutathione reductase (Manstein *et al.*, 1988), suggesting that the interaction between the nicotinamide ring and the flavin is similar at some point in the reaction cycle. However, the observed conformation of thioredoxin reductase in the crystal structure is inconsistent with the binding of NADPH in a productive mode.

The original structure determination of thioredoxin reductase was done using an active site mutant (Cys138Ser) that crystallizes more readily. Here, we describe details of the structure of wild-type *Escherichia coli* thioredoxin reductase, and show that it is essentially identical to that of the mutant enzyme. We have so far been unable to obtain crystals of the enzyme complexed with either NADPH or thioredoxin, and thus have no direct views of the enzyme in its reduced state. However, the structure of the $NADP^+$ complex clearly shows the location of this nucleotide in the enzyme and, together with other details of the structure, quite clearly implicates a large conformational change during catalysis.

2. Materials and Methods

(a) *Determination and refinement of the structures of the mutant (Cys138Ser) and wild-type forms of thioredoxin reductase*

Purified proteins were obtained as described by Prongay *et al.* (1989). Thioredoxin reductase contains a single redox-active disulfide at the active site, formed between Cys135 and Cys138. For reasons that are not clear, mutant forms of the protein where either cysteine is replaced by serine crystallize somewhat more readily than the wild-type enzyme. However, crystals of the wild-type enzyme can be obtained that are large enough for high resolution data collection (Kuriyan *et al.*, 1989), and crystals of all 3 forms of the enzyme are isomorphous (space group $P6_322$, $a = b = 123{\cdot}8$ Å, $c = 81{\cdot}56$ Å, 1 molecule in the asymmetric unit). X-ray data to 2·0 Å resolution were obtained for the (Cys138Ser) mutant at beamline X12-C, Brookhaven National Synchrotron Light Source, Upton, New York. A FAST area detector (Enraf-Nonius, Delft, The Netherlands) was used, with X-rays of wavelength 1·1 Å. Intensities were integrated over 0·1 deg. oscillations, using exposures of 10 to 20 s. A total of 135,848 measurements of 21,981 unique reflections to 2·0 Å resolution were merged with an overall $R_{symm}(I)$ of 6·4%. Data from 6 Å to 2·0 Å were used in the refinement, which proceeded using simulated annealing and least-squares optimization, essentially as described by Weis *et al.* (1990) and implemented in the program X-PLOR (Brünger, 1988). Examination of electron density maps and manual adjustments to the model were

carried out using the programs FRODO and O (Jones, 1985; Jones *et al.*, 1991). Details of the final model are given in Table 1.

X-ray intensity data collection for the wild-type crystals was carried out using a Rigaku R-AXIS IIC imaging phosphor area detector, mounted on a Rigaku RU200 rotating anode X-ray generator (Molecular Structure Corp., Houston). Typical crystal to detector distances and exposure times were 100 mm and 30 min, respectively, for 1 deg. oscillations. Data processing and reduction were done entirely by software provided by Rigaku. X-ray data collection statistics are reported in Table 1. Reflections between 6·0 and 2·1 Å resolution with $|F_{hkl}| > 2\sigma(|F_{hkl}|)$ were used for refinement, which started from the highly refined model for the (Cys138Ser) mutant. A difference electron density map showed the presence of a disulfide bond between Cys135 and Cys138. The stereochemical restraints were modified to account for the disulfide. Least-squares refinement (using the Powell optimization in X-PLOR (Brünger, 1988)) resulted in an *R*-factor of 19·2% from an initial value of 27·4%. The root-mean-square (r.m.s.) deviation from ideal values for bonds and angles is 0.008 Å and 2·3° respectively, (Table 1).

(b) *The structure of the enzyme/NADP⁺ complex*

Crystals of the mutant (Cys138Ser) enzyme were used for NADP⁺ binding studies since crystals of the wild-type enzyme were not available in large numbers. The crystals were stabilized in 40% polyethylene glycol (average molecular mass of 3·3 kDa) and 200 mM ammonium sulfate and were soaked in 10 mM NADP⁺ or 10 mM NADPH (Boehringer-Mannheim, Germany) for 1 week at 21 °C. Soaking crystals in higher concentrations of NADP⁺ or NADPH was attempted, but led to crystal cracking and/or loss of diffraction. No attempt was made to exclude air from the crystallization setups. Electron density maps obtained from soaks with either NADP⁺ or NADPH are similar, and we assume that the oxidized form is bound in either case and the structure described is for the NADP⁺ form. X-ray intensity data collection proceeded as for the wild-type enzyme (Table 1). Initial refinement was carried out using the model of the mutant enzyme from which the water molecules were deleted. A difference electron density map was calculated using this model and with coefficients $(|F_o|-|F_c|)e^{-i\alpha_c}$. Clear density features corresponding to bound cofactor were observed in the NADPH domain (Fig. 2). The NADPH domain of glutathione reductase (including the model for bound NADPH) was then superimposed on that of thioredoxin reductase, and it was clear that the density features in the difference map corresponded closely to the structure of NADP⁺ as observed in glutathione reductase (Pai *et al.*, 1988; Karplus & Schulz, 1989). As in glutathione reductase, density for the nicotinamide ring is very weak. A model for NADP⁺ was constructed based on the electron density and the co-ordinates of NADPH from glutathione reductase. This model was then used in a 2nd round of least-squares refinement using X-PLOR, with stereochemical parameters for NADPH kindly provided by Martha L. Ludwig and Carl C. Correll (University of Michigan, Ann Arbor, Michigan, U.S.A.). The water molecules were reincorporated into the model, deleting only those that were within 5 Å around the NADP⁺ molecule. At the end of this round of optimization, the *R*-factor was 18·2%. Analysis of temperature factors indicated that the occupancy of NADP⁺ is likely to be partial. The occupancy of the cofactor was set to 0·5, which results in temperature factors for the NADP⁺ that are comparable to those for side-chains observed to co-ordinate the cofactor. Despite the partial binding, density for the adenine and pyrophosphate components of NADP⁺ are unambiguous. The nicotinamide ring, however, is largely disordered and cannot be placed clearly in the electron density.

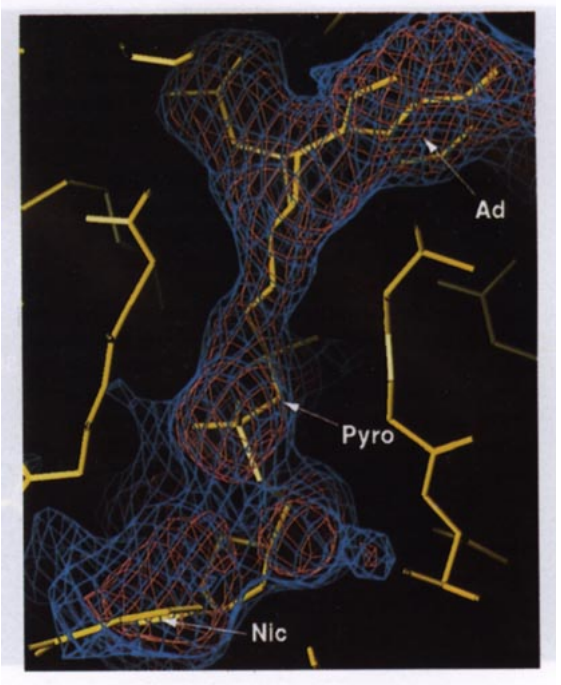

Figure 2. Electron density around the NADP⁺ molecule, shown in a chicken wire representation. The electron density map was calculated using $(|F_o|-|F_c|)e^{-i\alpha_c}$ coefficients, where $|F_o|$ is the observed structure factor amplitude and $|F_c|$ and α_c are the amplitudes and phases calculated from a model of the mutant enzyme that does not include the NADP⁺ model. The contours shown are at 1·0 (blue) and 2·0 (red) standard deviations above the mean value of the electron density in the map. The NADP⁺ molecule is shown as overlying yellow stick figures. Note that the nicotinamide ring is not well localized in the electron density.

All co-ordinates and X-ray structure factors have been deposited in the Protein Data Bank, Brookhaven National Laboratory, Upton, New York. Accession numbers for the Cys138Ser mutant are 1trb and 1trbsf.

3. Results

(a) *Quality of the structure*

The accuracy of the atomic model was first checked by calculating electron density maps using coefficients $(|F_o|-|F_c|)e^{-i\alpha_c}$, with various parts of the structure deleted from the model used for structure factor calculations (omit maps). Maps calculated using coefficients $(2F_o-F_c)e^{-i\alpha_c}$ show continuous density for the backbone of the entire molecule, except for one loop in the NADPH domain (residues 224 to 232). Very few side-chains

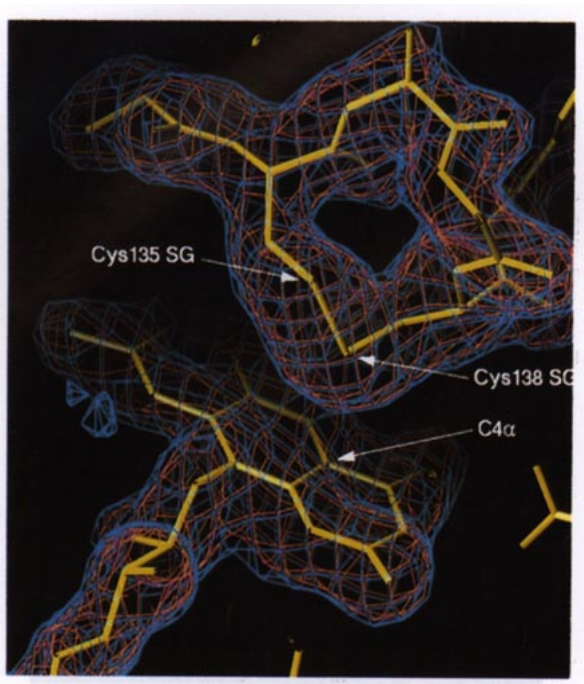

Figure 3. Electron density around the redox active disulfide, shown in a chicken wire representation. The electron density map was calculated using $(|F_o|-|F_c|)e^{-i\alpha_c}$ coefficients, where $|F_o|$ is the observed structure factor amplitude, and $|F_c|$ and α_c are the amplitudes and phases calculated from a model of the wild-type enzyme that does not include residues 134 to 139 (the redox active disulfide includes Cys135 and Cys138) and the FAD. The overlying stick figures in yellow represent the refined atomic co-ordinates. The redox active disulfide is indicated by its participating sulfur atoms. Also indicated is the C4α atom of the FAD that is involved in thiolate adduct formation.

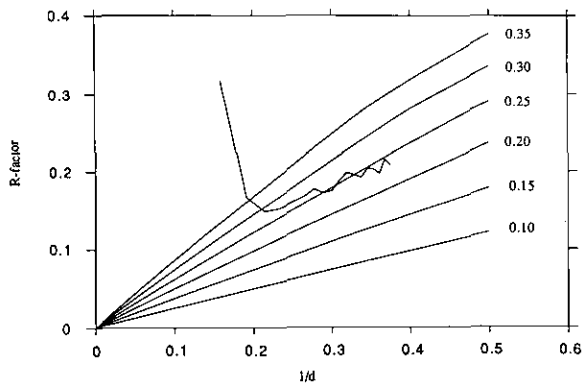

Figure 4. *R*-factor *versus* resolution ($1/d$) for the (Cys138Ser) enzyme. The lines corresponding to the upper estimates of errors in atomic co-ordinates are taken from Luzzati (1952). d is the Bragg spacing in Å.

are in poor density, and these are arginine and lysine residues on the surface of the molecule (residues 184, 188, 189). A representative omit map, obtained by deleting the redox active cysteines and intervening residues (135 to 138) is shown for the wild-type structure in Figure 3. This map shows strong density for the two sulfur atoms in the disulfide bridge, in contrast to maps calculated for the Cys138Ser mutant, which clearly show the lack of the disulfide bond.

The dependence of the *R*-factor on resolution is shown in Figure 4 for the Cys138Ser mutant, and implies an upper limit of about 0·25 Å for the overall error in atomic positions (Luzzati, 1952). The isotropic temperature factor profile and solvent accessibility for the enzyme is shown in Figure 5. The highest temperature factors occur in the loops connecting secondary structural elements. However, temperature factors in a region of the NADPH domain beween residues 176 and 232 are significantly higher on average than in other regions of the structure. Notably residues 223 to 232 corresponding to a disordered surface loop in the NADPH domain show very high mobility. This loop is not close to either the disulfide or the NADPH binding site. Excluding this region (223 to 232) of high mobility, the average *B*-factor for main-chain atoms is 18·9 Å^2. A Ramachandran plot for both glycine and non-glycine residues of the mutant enzyme is shown in Figure 6 (Ramachandran & Sasisekharan, 1968). Only three of the (ϕ,ψ) combinations fall outside the conformational energy map for glycine and alanine tripeptides (Brant & Schimmel, 1967; Peters & Peters, 1981). These residues are Thr47, Asp58 and Lys184. Except for Lys184, for which the density is poor, all other residues are unambiguously defined by the electron density.

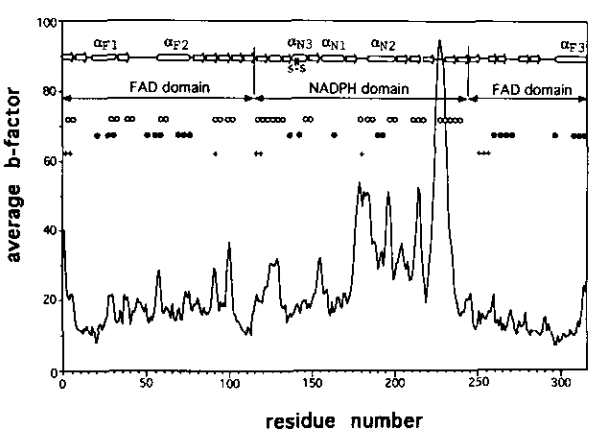

Figure 5. Average isotropic temperature factors for protein backbone *versus* residue number for the (Cys138Ser) mutant enzyme. *B*-factors are in Å^2. The sequence boundaries of the 2 domains are indicated. Secondary structure elements are reported with arrows indicating β-sheets and cylinders indicating α-helices. Circles indicate regions of the structure with solvent accessibility of side-chain atoms above 20 Å^2. Filled circles indicate regions of the structure involved in dimer formation. (+) indicates regions of the structure involved in crystal contacts and not in dimer formation.

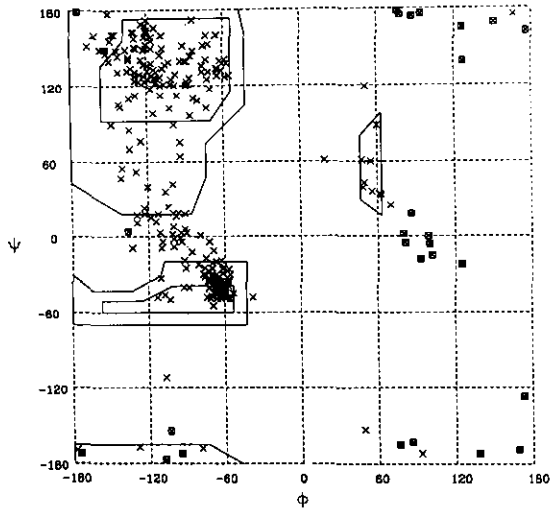

Figure 6. Conformational angles for the (Cys138Ser) mutant enzyme (Ramachandran plot). The non-glycine residues are indicated by x and the glycines by crossed squares.

(b) *Comparison of the structures of wild-type enzyme and Cys138Ser mutant*

The structures of the wild-type and mutant enzyme are essentially identical, except in the immediate vicinity of the changed residue. The overall r.m.s. deviation in backbone and side-chain atom positions for the two structures are 0·15 and 0·31 Å, respectively. There is little structural difference (r.m.s. deviation in backbone of 0·09 Å) in the geometry of the region corresponding in the wild-type to the redox active disulfide. The only significant shift is for the hydroxyl group of Ser138 in the Cys138Ser mutant structure, which moves by 0·4 Å, compared to the equivalent sulfur atom in the Cys138 side-chain of the wild-type enzyme.

(c) *Structure of the thioredoxin reductase monomer*

A diagram showing the organization of secondary structure elements is presented in Figure 7 and a schematic representation of the three-dimensional backbone fold of the molecule is shown in Figure 8

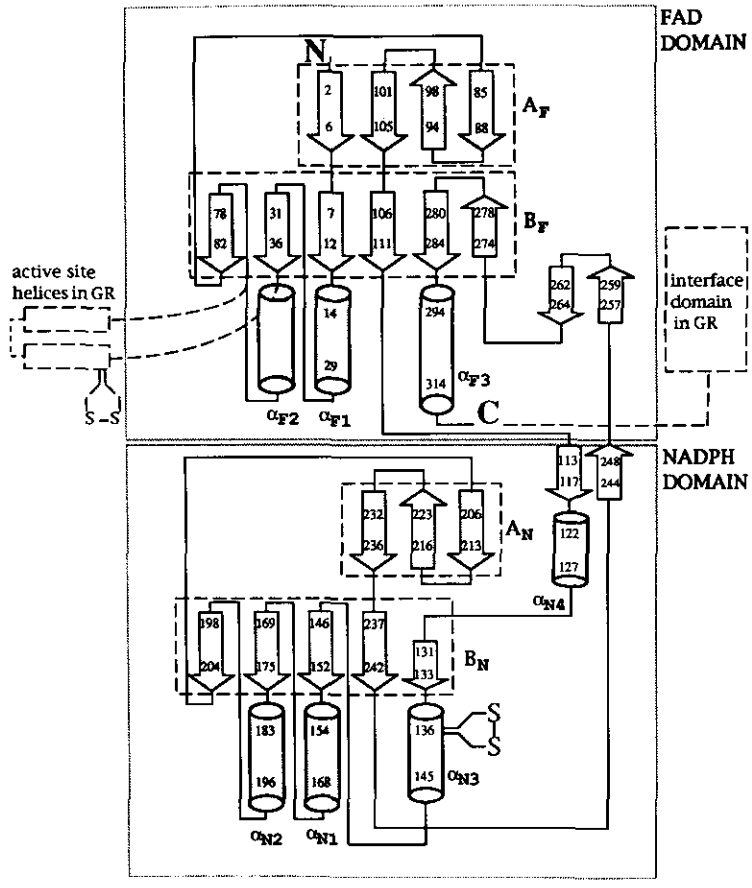

Figure 7. Schematic drawing of the secondary structure of thioredoxin reductase. α-Helices are shown as cylinders and β-strands as arrows. The intervening loops are indicated with continuous lines. The numbers at the beginning and the end of the secondary structural elements are the sequence numbers of the boundary residues. The FAD and NADPH domains are boxed. Elements of the secondary structure in the 2 domains that can be aligned in 3 dimensions are shown with shaded arrows or cylinders. Dashed boxes indicate sheets A and B in the 2 domains, with sheets A and B indicated as A_F and B_F *in the* FAD *domain, and* A_N *and* B_N *in the* NADPH *domain. Likewise, the helices are labeled* α_{F1}, α_{F2}, α_{F3} *in* the FAD domain, and α_{N1}, α_{N2}, α_{N3}, α_{N4} in the NADPH domain. Note that for clarity, the antiparallel β-sheet that connects the FAD domain and the NADPH domain is included in the NAPDH domain. Broken lines indicate structural elements of glutathione reductase that do not have counterparts in thioredoxin reductase.

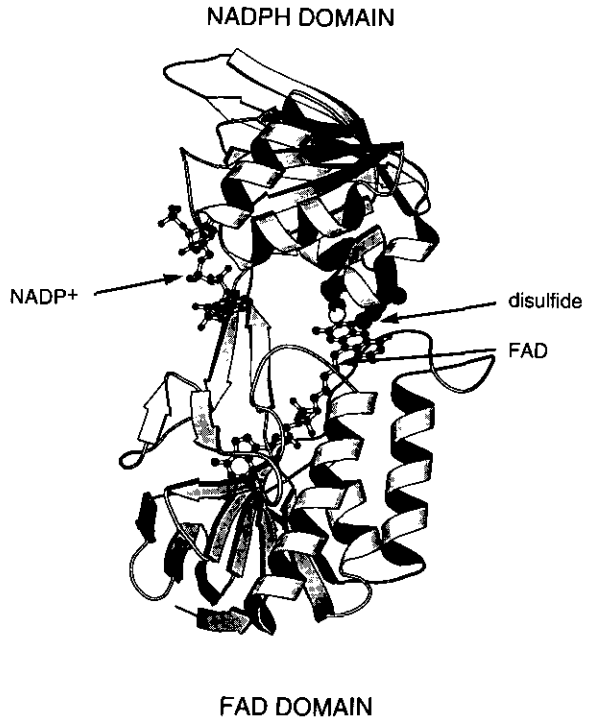

Figure 8. Schematic ribbon drawing (Kraulis, 1991) of the enzyme monomer showing the position of $NADP^+$ relative to the positions of the 2 other elements of the active site, FAD and redox active dithiol. The α-helices are shown as ribbon helices, β-strands as ribbons with arrows, and loops are drawn as single lines. The redox active dithiol is indicated as filled circles, and the FAD and $NADP^+$ as balls and sticks. Note that the orientation of the molecule is different from that presented in Fig. 13: the β-sheet connecting the FAD and NADPH domains is here clearly visible. Note that the nicotinamide ring of $NADP^+$ is not well localized in the electron density.

(Kraulis, 1991). The molecule is clearly comprised of two compact sub-structures, which correspond to the FAD and NADPH binding domains. The FAD domain contains two non-contiguous regions of sequence (residues 1 to 112 and residues 249 to 320), and the NADPH domain (residues 113 to residue 248) represents an insertion in the FAD domain. This architecture closely resembles that of glutathione reductase, except that the interface domain is lacking. Another important difference is the location of the redox active disulfide bond, which in thioreodoxin reductase is in the NADPH domain.

In each domain there are two β-pleated sheets, which are designated A and B in Figure 7. Parts of sheets A and B of the NADPH and FAD domains of thioredoxin reductase have extensive similarities (see Fig. 7). Residues 7 to 111 of the FAD domain and residues 146 to 242 of the NADPH domain form the major part of sheets A and B in both domains. The structures of these regions are similar, except for an insertion in the loop between residues 37 and 59 in the FAD domain. Interestingly, this loop is an essential structural element of the dimer interface (see Fig. 11(a)). When the residues of this loop are excluded from the alignment of the two regions, the

Table 2
Occurrence of 3_{10}-helices in the Cys138Ser mutant

Residue	$\phi°$	$\psi°$
Gln42	−61	−24
Leu43	−75	−17
Thr44	−72	−4
Thr45	−101	2
Gly140	−61	−36
Phe141	−70	−21
Phe142	−62	−26
Tyr143	−104	24
Ala250	−58	−38
Ileu251	−57	−26
Phe252	−100	−2
Asp286	−67	−20
Val287	−61	−25
Met288	−118	15

r.m.s. deviation in C^α positions is 2·3 Å. Both regions contain β-α-β-α-β folds (residues 7 to 82 of the FAD domain, and residues 146 to 204 of the NADPH domain) or "Rossman folds" (Rossmann *et al.*, 1975) that form the binding sites for both dinucleotides. The observed similarities between the FAD and NADPH domains of thioredoxin reductase are consistent with the suggestion of Schulz (1980) that the two domains have arisen by gene duplication.

The domains are not, however, strictly similar in their secondary structural topology. One strand (residues 2 to 6) is added to the conserved part of sheet A of the FAD domain, and two antiparallel strands (residues 274 to 284) to the conserved part of sheet B of the same domain, and one short strand (residue 131 to 133) runs parallel to the conserved part of sheet B of the NADPH domain. These features extend sheet A and sheet B of the FAD domain to a four and six-stranded β-sheet, respectively, and sheet B of the NADPH domain to a five-stranded β-sheet.

The FAD domain also contains a two-stranded β-meander (residues 257 to 264), which forms part of the dimer interface (see Fig. 11(b)), as well as an extended α-helix at the C-terminal end of the molecule (residues 294 to 314), which also contributes residues to the dimer interface. The NADPH domain contains a small helix (residues 122 to 127), which seems to position the redox active disulfide. The helix that contains the redox active disulfide (residues 136 to 145) is in a 3_{10} conformation at its C terminus. 3_{10} helices are also observed in sections of the sequence comprising residues 42 to 45, residues 250 to 252 and residues 286 to 288 (Table 2). Interestingly, three of these 3_{10} helices are conserved in glutathione reductase. The one non-conserved 3_{10} helix (residues 42 to 45) corresponds to a long α-helix in glutathione reductase that contains the redox active disulfide bond of that enzyme. Finally, the connection between the two domains of thioredoxin reductase consists of a short antiparallel β-sheet, which comprises residues 113 to 117 and 244 to 248.

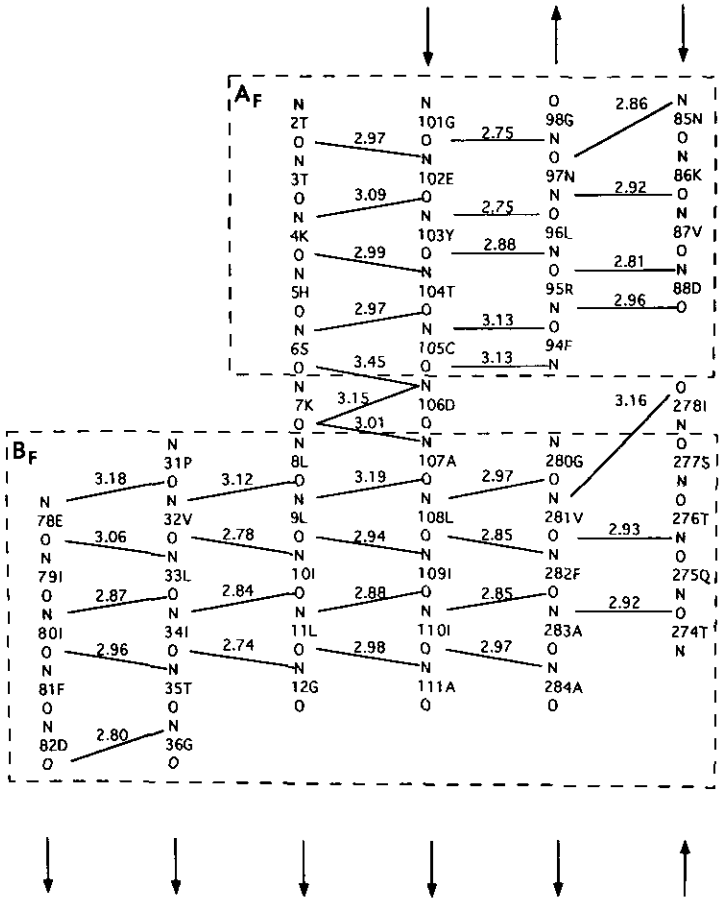
A_F
B_F
2T
3T
4K
5H
6S
7K
101G
102E
103Y
104T
105C
106D
98G
97N
96L
95R
94F
85N
86K
87V
88D
278I
277S
276T
275Q
274T
31P
32V
33L
35T
36G
8L
9L
10I
11L
12G
107A
108L
109I
110I
111A
280G
281V
282F
283A
284A
78E
79I
80I
81F
82D
2.97
3.09
2.99
2.97
3.45
3.15
3.01
2.75
2.88
3.13
3.13
2.86
2.92
2.75
2.81
2.96
3.16
3.18
3.12
3.19
2.97
3.06
2.78
2.94
2.85
2.93
2.87
2.84
2.88
2.85
2.92
2.96
2.74
2.98
2.97
2.80

(a)

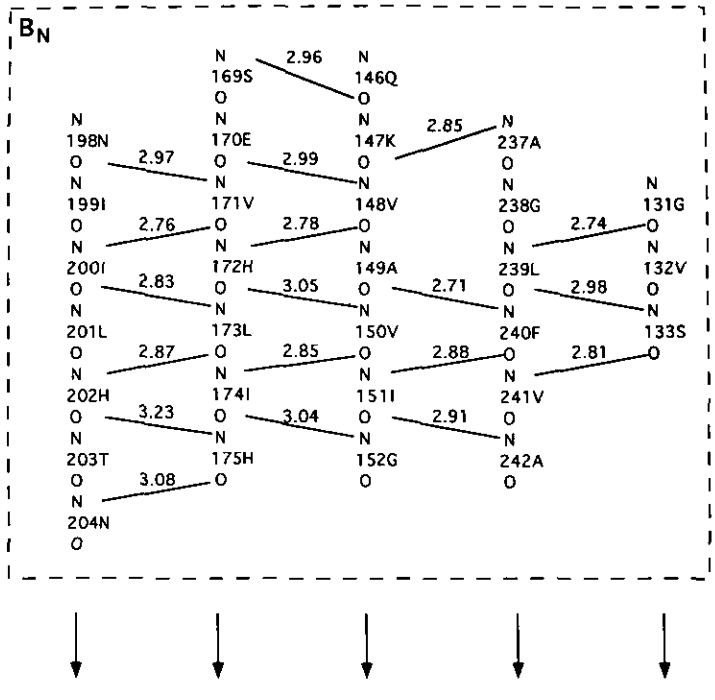
B_N
169S
146Q
198N
170E
147K
237A
199I
171V
148V
238G
131G
200I
172H
149A
239L
132V
201L
173L
150V
240F
133S
202H
174I
151I
241V
203T
175H
152G
242A
204N
2.96
2.97
2.99
2.85
2.76
2.78
2.74
2.83
3.05
2.71
2.98
2.87
2.85
2.88
2.81
3.23
3.04
2.91
3.08

(b)

Fig. 9.

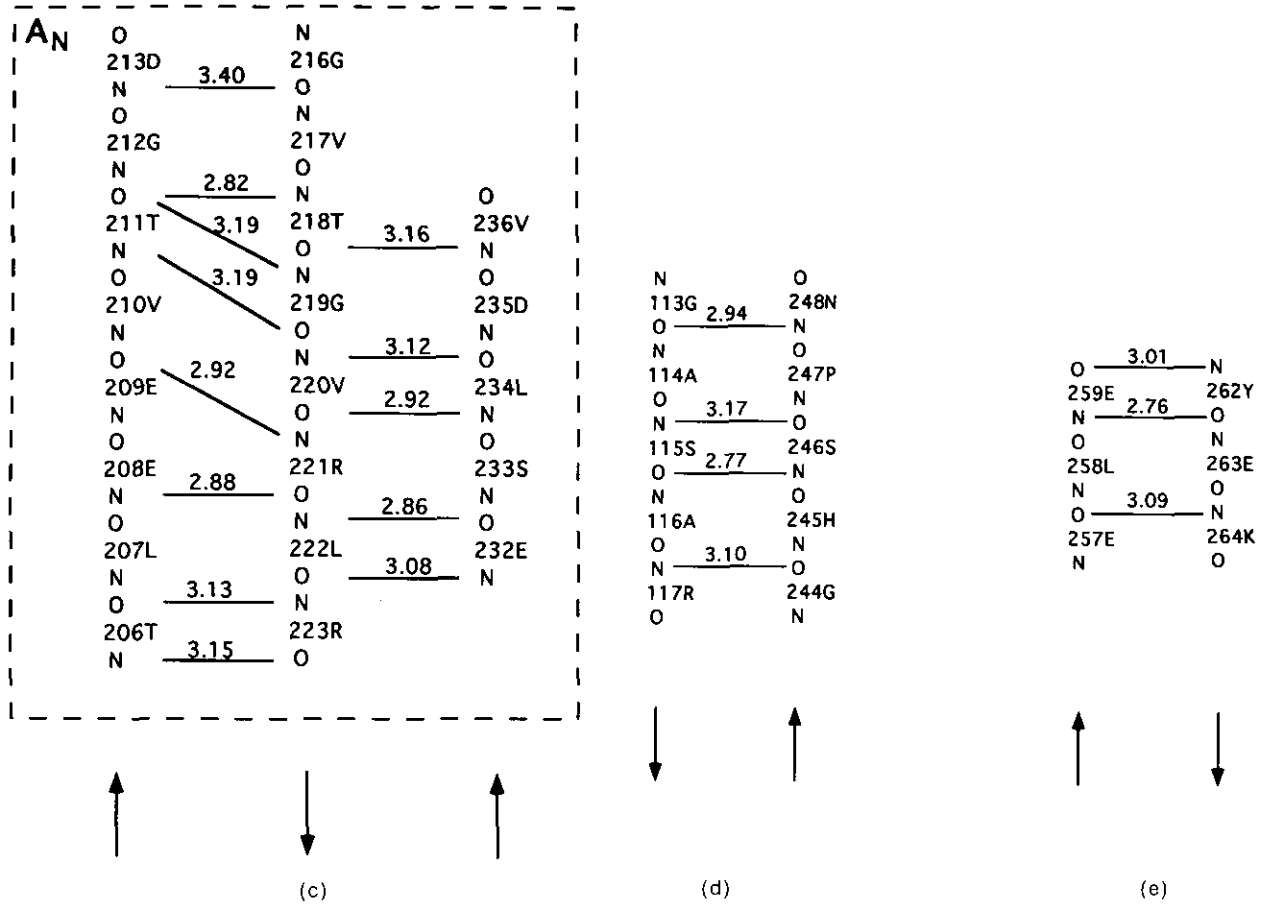

Figure 9. Representation of the β-structures. Hydrogen bonds are indicated with continuous lines connecting donors and acceptors, and their lengths are given in Å. Strand polarities are indicated with arrows. (a), The sheet structure of the FAD domain. (b). The parallel β-structure of the NADPH domain. (c), The antiparallel β-structure of the NADPH domain. (d), The 2-stranded structure connecting the FAD and NADPH domains. (e), The antiparallel β-meander of the FAD domain.

The detailed hydrogen bonding geometries of the β-sheets are illustrated in Figure 9. The total number of residues found in helices or sheets is 211 of 316, or 67%, of which 42% are found in helices. Approximately 33% of the polypeptide chain occurs in the form of loops and turns connecting α-helices and β-sheets. There are 12 reverse turns with a 1–4 hydrogen bond, listed in Table 3.

The NADPH domain and the FAD domain do not interact extensively in the monomer. Only two hydrogen bonding interactions involve residues of the NADPH domain and residues of the FAD domain: one between Gly129 and Thr47 and another between Arg130 and Glu48, the latter forming an ion pair. Other contacts between the two domains are mediated through five water molecules. Most of the other intramolecular ion pairs (Table 4) occur at the protein surface. One ion pair (Asp55/Arg67) seems to play a role in structuring a loop of the FAD domain involved in dimerization (see Figure 11(a)).

(d) *Dimer structure*

In contrast to the similarity in tertiary structure, the dimeric form of thioredoxin reductase is completely different from that of glutathione reductase. Schematic diagrams of the dimer structure of glutathione reductase and thioredoxin reductase are presented in Figure 1. Dimer formation in glutathione reductase involves an interlocking of the interface domains, with each one making contacts with the interface and FAD domains of the other molecule and forming the deep crevices that are the

Table 3
1-4 Hydrogen bonded reverse turns in the Cys138Ser mutant

Residues	$\phi 2°$	$\psi 2°$	$\phi 3°$	$\psi 3°$	Type
38 E–41 G	−70	117	103	−15	II
52 W–55 D	−64	128	100	0	II
127 F–130 R	−55	128	80	2	II
141 F–144 R	−62	−26	−104	24	I
143 Y–146 Q	−58	127	70	25	II
213 D–216 G	−56	−30	−88	−40	III
252 F–255 Q	−61	132	81	−5	II
259 E–262 Y	49	39	93	−18	I′
272 N–275 Q	−70	−26	−94	3	I
278 I–281 V	−58	127	100	−6	II
285 G–288 M	−67	−20	−61	−25	III
286 D–289 D	−61	−25	−118	15	I

Table 4
Ion-pairs within the Cys138Ser monomer with separation given in Å

A. *Ion-pairs within the FAD domain*		
5 H NE2	106 D OD1	2·9
55 D OD1	67 R NH2	3·0
308 D OD1	311 R NH1	2·6
55 D OD2	67 R NH1	2·6
B. *Ion-pairs between the FAD and NADPH domain*		
130 R NH1	48 E OE2	3·2
C. *Ion-pairs within the NADPH domain*		
125 E OE1	128 K NZ	3·2
147 K NZ	170 E OE1	3·1
147 K NZ	170 E OE2	3·0
170 E OE2	172 H NE2	2·7
205 R NH2	232 E OE2	2·9
209 E OE2	221 R NE	3·0
209 E OE2	221 R NH1	2·8

Table 5
Hydrogen bonds that stabilize the Cys138Ser dimer enzyme complex with distances given in Å

A. *Interactions between FAD domains*		
23 Y OH	294′ Q OE1	2·7
26 R NE	50′ E OE2	3·1
26 R NH1	50′ E OE2	3·1
50 E O	71′ H NE2	2·8
54 G O	67′ R NH2	3·2
54 G N	71′ H NE1	3·0
56 P O	74′ K NZ	2·7
57 N OD1	74′ K NZ	3·1
259 E OE1	270′ H NE2	2·8
259 E OE2	270′ H NE2	3·0
267 S OG	267′ S OG	2·9
292 Y OH	273′ A N	3·2
308 D OD1	292′ Y OH	2·7
308 D OD2	292′ Y OH	3·4
B. *Interactions between FAD and NADPH domains*		
26 R NH1	138′ S O	2·9
26 R NH2	138′ S O	2·8
28 N OD1	144′ R NE	3·0
166 N O	28′ N ND2	2·8
189 R NE	314′ D O	2·8
189 R NH1	314′ D OD1	3·0
189 R NH2	314′ D OD1	2·5
193 K NZ	314′ D OD1	3·2
193 K NZ	314′ D OD2	3·1
310 E OE1	166′ N OD1	3·2
314 D OD1	166′ N OD1	3·0

binding site of glutathione. In thioredoxin reductase, dimer formation involves primarily the FAD domain and depressions at the dimer interface are very shallow.

Residues involved in dimerization through hydrogen bonding are listed in Table 5. There is an extensive network of residues involved in dimer contacts. Most contacts are provided by the FAD domains of each monomer. Three α-helices (α_1, α_2 and α_3) in the FAD domain provide half of the residues of the FAD domain involved in dimerization (compare with Fig. 10(c)). Two loops (37 to 59 and 265 to 273) provide most of the remaining contributing residues of this domain. These two loops are clearly visible at the surface of the structure and form two arms that seem to take hold of the other monomer (Fig. 10). Detailed illustrations of the contribution of these two loops to the dimer interface are given in Figure 11. Other residues involved in dimer stabilization are contributed by the NADPH domain through contacts with the FAD domain of the other monomer. This type of contact is not observed in glutathione reductase. A total of 28 water molecules are involved in stabilizing the molecule at the dimer interface and do not appear in clusters as in glutathione reductase. In glutathione reductase, the largest solvent cluster is at the dimer interface and contains 104 molecules (Karplus & Schulz, 1987).

The total interface area buried upon dimerization is 2900 Å^2, which is smaller than the dimer interface surface of glutathione reductase (3590 Å^2) (Richards, 1977; Janin & Chothia, 1990). However, this amounts to nearly 21% of the total accessible surface of the monomer instead of 15% in glutathione reductase. In thioredoxin reductase, the interface area can be subdivided into six regions shown in Figure 10. Two involve contacts between the NADPH domain of one monomer with the FAD domain of the other monomer and are shown in the upper right and lower left circles of Figure 10(a). The four other parts are indicated in the upper central and lower central circles of Figure 10(a) and 10(b) and include an extensive and continuous interface between the two FAD domains. The circles shown in Figure 10(a) and 10(b) indicate regions where surface loops from the two FAD domains interact with each other. These circles define upper and lower contact areas which are equivalent since they are related by the 2-fold symmetry axis which is in the middle of the dimer and perpendicular to the plane of view in Figure 10. There is a hydrophobic core formed at the interface, between the two central circles in the Figure, and this involves close packing of the side-chains of Pro15, Pro53, Trp52, Leu64, Met68, Ile296 and Ala299 with each other and with their symmetry-related equivalents. This hydrophobic core is a consequence of dimer formation, and is distinct from the hydrophobic cores that are within each separate domain.

The surface of the regions involved in contacts is estimated to be 504 Å^2 for the NADPH/FAD upper or lower contact area and 945 Å^2 for the FAD/FAD upper or lower contact area. Therefore, the FAD/FAD domain interactions contribute most of the dimer formation surface (65%). Interestingly, the contribution of NADPH/FAD domain interactions to the dimer interface is not negligible. However, one can note that the dimer interface region involving the NADPH domain is located opposite the site of NADPH binding and therefore does not interfere with NADPH binding.

(e) *Elements of the active site*

The catalytic properties of thioredoxin reductase distinguish it as a unique member of the family of

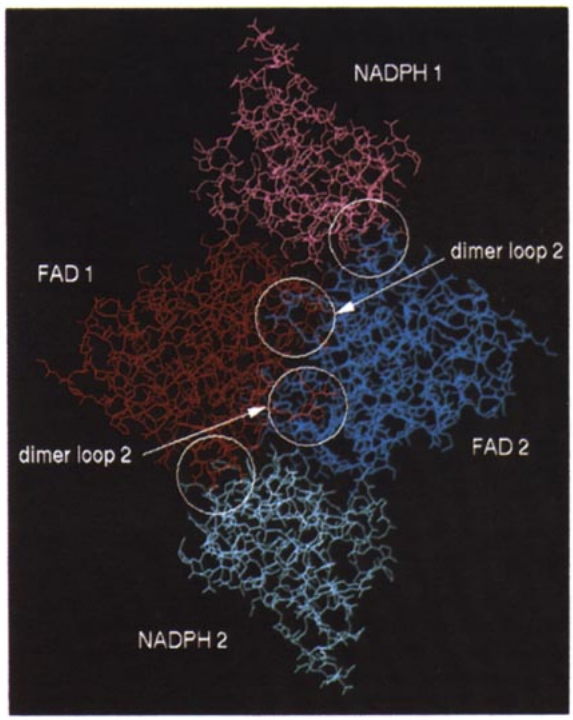

(a)

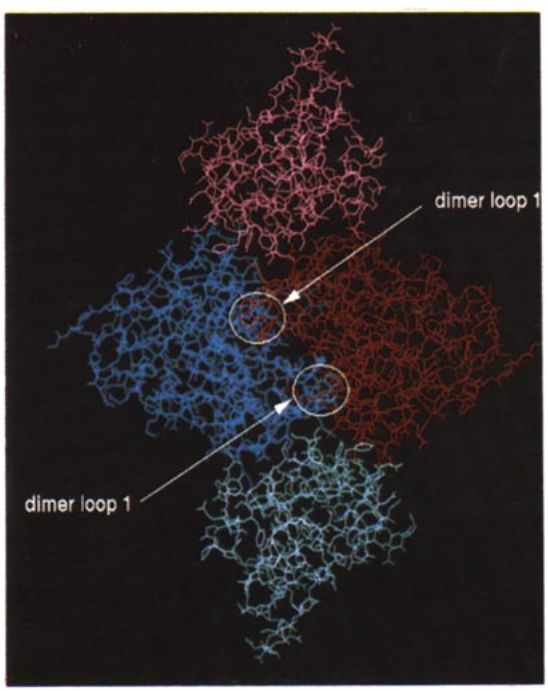

(b)

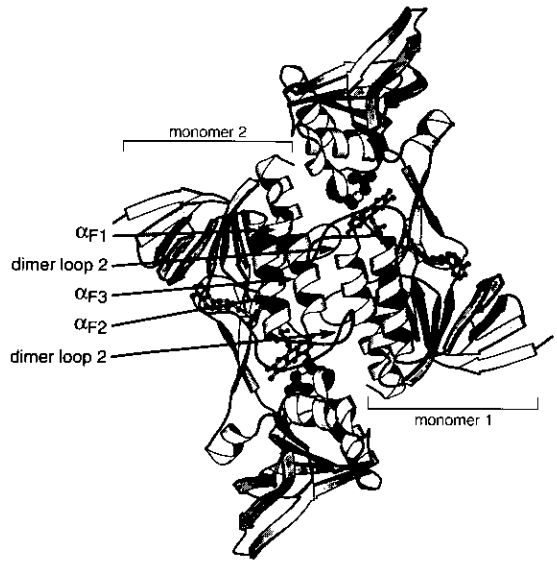

(c)

Figure 10. The enzyme dimer looking down the 2-fold axis. The 2-domain structure of each monomer is indicated in red (FAD domain) and pink (NADPH domain) for monomer 1, and dark blue (FAD domain) and light blue (NADPH domain) for monomer 2. (a), Four circles indicate regions of contact. The 2 most central circles labeled dimer loop 2 indicate 1 of the 2 loops involved in dimer formation. Detail of the interactions contributed by this structure is presented in Fig. 11(b). (b), The dimer was rotated 180° around an axis perpendicular to the 2-fold symmetry axis of the molecule and shows in the 2 circles the 2nd loop involved in dimer formation. Detail of the interactions contributed by this loop is presented in Fig. 11(a). (c), Ribbon drawing of the enzyme dimer (Kraulis, 1991). α-Helices are shown as ribbon helices, β-strands as ribbons with arrows, and loops are drawn as single lines. The redox active dithiol is indicated as filled circles and the FAD as balls and sticks.

flavoprotein disulfide reductases. For instance, thioredoxin reductase has an FAD with a redox potential which is less negative than that of other members of the family and which is essentially the same as that of the dithiol/disulfide couple. This results in an enzyme which is able to undergo 4-electron reduction (O'Donnell & Williams, 1983). Also, analysis of thioredoxin reductase variants mutated at the redox active cysteines (Cys138Ser and Cys135Ser) resulted in the identification of Cys138 as the thiol interacting closely with the flavin and it was proposed that the other thiol (Cys135), by analogy to glutathione reductase and lipoamide dehydrogenase, was the interchange thiol. Both mutants retained some catalytic activities, suggesting that both cysteine residues are relatively close to the flavin and that thioredoxin reductase has a more open active site than glutathione reductase (O'Donnell & Williams, 1985; Prongay *et al.*, 1989; Prongay & Williams, 1990, 1992). The analysis of the X-ray structure below discusses these points in detail.

(i) *The FAD binding site*

The FAD group is very well defined in the electron density map and its conformation is virtually identical to that of FAD in glutathione reductase. The FAD molecules in glutathione reductase and thioredoxin reductase superimpose with a r.m.s. deviation between the two structures of only 0·36 Å. Also, as mentioned before, the binding site of the FAD molecules do not significantly differ from that

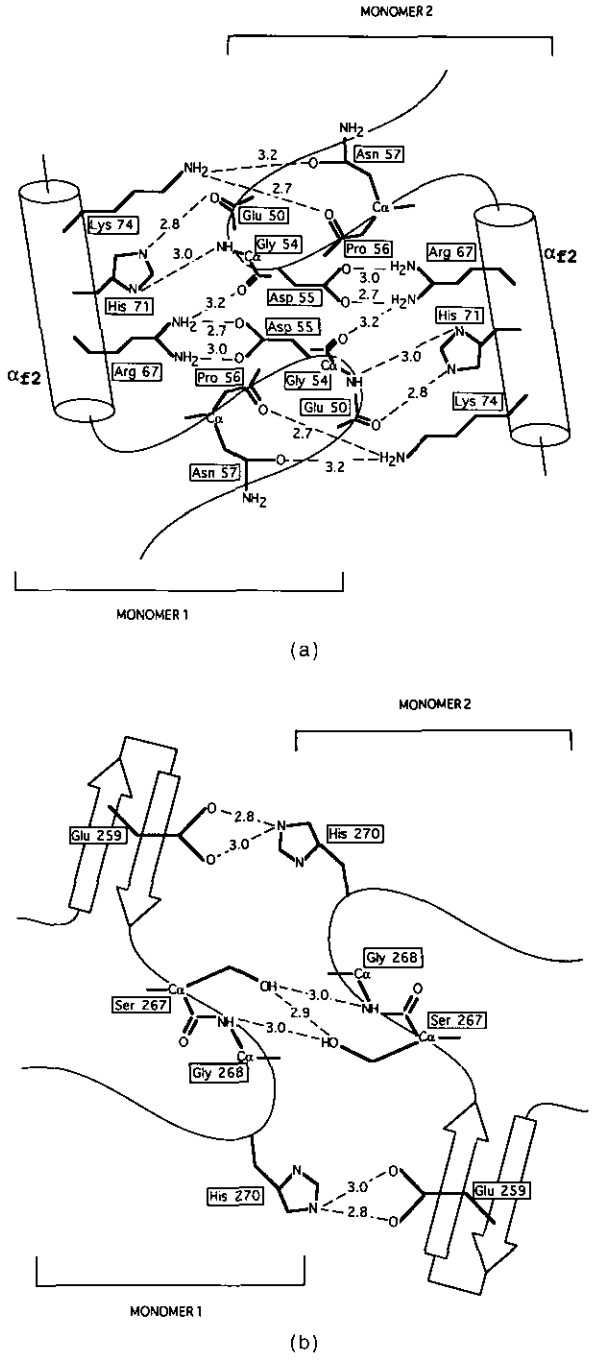

Figure 11. Schematic representation of the 2 large loops involved in dimer formation. (a), Dimer loop 1. (b), Dimer loop 2.

observed in glutathione reductase (Schulz *et al.*, 1982). The hydrogen bonding interactions between protein and FAD are shown in Figure 12(a). The FAD binds in a rather elongated conformation with the flavin portion reaching out towards the NADPH domain, but deeply buried in the protein, while the adenine portion extends to its surface. The isoalloxazine ring system is located at the α-helix side of the parallel β-sheet, while the adenine part is at the other side of this sheet (Fig. 8).

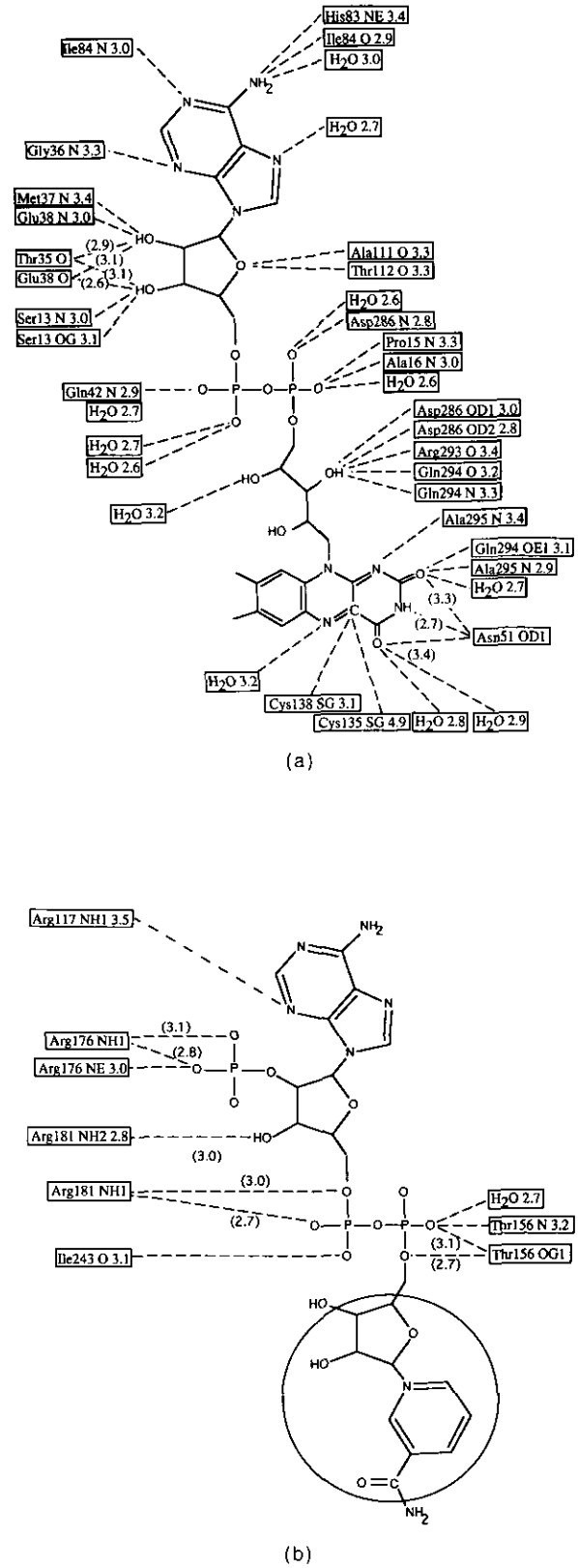

Figure 12. Schematic drawing of the FAD (a) and $NADP^+$ (b) molecules. Residues interacting with FAD and $NADP^+$ are in boxes. Also in boxes is the type of atom involved in the interaction as well as the distances in Å between donors and acceptors. Broken lines indicate hydrogen bonding. When the same atom contributes 2 interactions with the dinucleotide, the distances are indicated on the broken line. The circle indicates disorder.

As in glutathione reductase, the *si*-face of the isoalloxazine ring system is covered by a polypeptide chain. However, in glutathione reductase this segment of the chain contains the redox active disulfide and is part of an extended helix. In thioredoxin reductase this segment of the chain is part of a short 3_{10} helix that does not contain the redox active disulfide, which is, instead, in the NADPH domain on the *re*-face of the isoalloxazine ring system (Fig. 3).

A common feature of glutathione reductase and other flavoenzymes, which is also seen in thioredoxin reductase, is the involvement of an extended C-terminal helix (helix α_{F3} in thioredoxin reductase) in stabilizing the N1-O2$^{\alpha}$ region of the ring system. The helix dipole field may influence the charge distribution in the ring and therefore affect the catalytic properties of the enzyme (Hol *et al.*, 1978). Also, as observed in glutathione reductase and *p*-hydroxybenzoate hydroxylase, a peptide NH-group in the first turn of this helix (residue 295) forms hydrogen bonds with N1 and O2$^{\alpha}$ of the isoalloxazine ring system. The ribitol chain interacts with residues (Asp286, Arg293 and Gln294) in the loop connecting this C-terminal helix.

As in glutathione reductase, the N-terminal region of helix α_{F1} of thioredoxin reductase (residue 14 to 29) is very close to the pyrophosphate, and its dipole field may stabilize the negative charge of this group (Hol *et al.*, 1978). As in glutathione reductase, and unlike *p*-hydroxybenzoate hydroxylase, there are no positively charged side-chains to compensate the negative charge of the pyrophosphate of the FAD (Wierenga *et al.*, 1979, 1983).

Another feature that is common to glutathione reductase and *p*-hydroxybenzoate hydroxylase is the stabilization of the adenine ribose moiety. Backbone atoms of residues in the second strand of the parallel β-sheet of the Rossman fold (Thr35) and in the following loop (Met37, Glu38) contribute binding interactions with the ribose, while the loop connecting this sheet to the contiguous antiparallel β-sheet is involved in interacting with the adenine (His83 and Ile84).

(ii) *The NADPH binding site*

One can easily recognize in the secondary structure elements of the NADPH domain of thioredoxin reductase the typical fold which makes up the dinucleotide binding site: the β-α-β-α-β or Rossman fold (residue 146 to 204) with a β-strand added to it (residues 237 to 242) and an additional antiparallel β-sheet (residues 206 to 236). This fold is very conserved both in thioredoxin reductase and glutathione reductase.

Difference map calculated using the $(|F_o|-|F_c|)e^{-i\alpha_c}$ coefficients, where the structure factor F_c is calculated from the model for the uncomplexed enzyme and F_o is that measured for the NADP$^+$ complex, revealed strong density around the predicted dinucleotide binding site (Fig. 2). The observed mode of binding is virtually identical to that seen in glutathione reductase. As found in glutathione reductase, NADP$^+$ binds in a well-defined manner to the enzyme at the adenine end, but the observed density is poor for the nicotinamide ring. During refinement, occupancy for the entire cofactor was set to half the occupancy of the other atoms in the protein and that of the nicotinamide moiety set to zero (that is, the nicotinamide ring was not included in the crystallographic term). The average temperature factor of the NADPH domain is similar in the structures with or without NADP$^+$.

Hydrogen bonding interactions between the protein and the NADP$^+$ molecule are presented in Figure 12(b). The region of the protein around the 2′-phosphate is positively charged with one arginine residue (Arg176) stabilizing the negative charge of the phosphate, and another arginine residue (Arg181) interacting with the pyrophosphate and the adenine ribose. These residues are contributed by the loop of the Rossman fold connecting the middle strand of the fold and the subsequent helix. A similar pattern is observed in glutathione reductase where two arginine residues (218 and 224) interact with the phosphate, and are involved in neutralizing the pyrophosphate and stabilizing the adenine ribose. The first helix of the β-α-β-α-β motif contributes its dipole field to the stabilization of the pyrophosphate. The interaction between the protein and the nicotinamide moiety is not clear because of the poor density around the nicotinamide ring. Unlike in glutathione reductase, where there are as many hydrogen bonds *via* water molecules as there are directly with the protein, in thioredoxin reductase only one well-defined water molecule is observed and it interacts with the pyrophosphate. Finally, helix 294 to 314 (α_{F3}), which plays an important role in the interaction with the FAD, does not have a counterpart in the NADPH domain. Instead, helix α_{N3} plays a very different role and presents the redox active disulfide to the isoalloxazine ring system.

The observed binding mode for NADP$^+$ places the nicotinamide ring on the surface of the protein, where it is more than 17 Å from the flavin (Fig. 8). It is unlikely that hydride transfer can occur directly over this distance, implying that this is a non-productive binding mode. It is clear that the binding of NADP$^+$ or NADPH at the concentration used for the experiments described here is insufficient to trigger a conformational change in this crystal form of oxidized thioredoxin reductase. However, the use of higher concentration of NADPH resulted in crystals cracking, which might indicate a reorganization of the domains upon full occupancy binding of the dinucleotide.

(iii) *The redox active disulfide site and potential interactions with thioredoxin*

A striking difference between glutathione reductase and thioredoxin reductase, which was apparent as soon as the sequence of thioredoxin reductase was known (Russel & Model, 1988), is that the NADPH domain and not the FAD domain contributes the

active dithiol site in thioredoxin reductase. Figure 3 shows that the disulfide stacks against the *re* side of the isoalloxazine ring system. The orientation of the disulfide bond with respect to the flavin is different in thioredoxin reductase and glutathione reductase: it is more parallel to the isoalloxazine ring system in the former, while it is nearly perpendicular in the latter. However, one can clearly recognize the difference between the two thiols: one (Cys138) is nearer the C4^{x} atom of the FAD than the other (3·0 Å for Cys138 and 4·8 Å for Cys135) and is therefore the more likely candidate to form the covalent thiolate adduct with the flavin after reduction (Prongay *et al.*, 1989; Prongay & Williams, 1990, 1992). The conformation of the 17 atoms making up the disulfide bonded ring closely resembles that seen in thioredoxin with an r.m.s. of 0·22 Å, despite the fact that the structural scaffoldings are quite different in the two proteins.

In lipoamide dehydrogenase and glutathione reductase, an acid/base catalyst is involved in the reaction mechanism. An active site histidine residue in lipoamide dehydrogenase functions as a base catalyst to deprotonate dihydrolipoamide for nucleophilic attack on the enzyme disulfide (Matthews & Williams, 1976), while a histidine residue (His467) in glutathione reductase acts as an acid catalyst to protonate the first molecule of glutathione (Wong *et al.*, 1988). These acid/base catalysts also form ion-pair partners for the nascent thiolate in the apolar milieu of the active site. In thioredoxin reductase, an active site base has been implicated (O'Donnell & Williams, 1983). His245 is the only histidine residue near the disulfide bond, but it is about 7·3 Å from Cys135. Although it was suggested that it could be the base catalyst involved in the reaction (Kuriyan *et al.*, 1991*b*), site directed mutagenesis has shown that this is unlikely to be the case (S. B. Mulrooney and C. H. Williams, Jr, personal communication). His245 is homologous to Arg291 in glutathione reductase and may play a role in influencing the polarity near the FAD (Pai & Schulz, 1983). Arginine 293 is located within 7·5 Å of Cys135 and could also provide potential stabilization for the thiolate. Asp139 is the nearest potential acid/base catalyst to the redox active disulfide (6·2 Å from Cys135 and 5·1 Å for Cys138). Mutagenesis of Asp139 to Glu or Asn reduces enzyme activity by 62 or 98%, respectively; an Asp139Leu mutant is without any measurable activity. All three of these altered forms have normal transhydrogenase activity showing that catalysis involving only the FAD is unimpaired. Asp139Asn is reduced at the same rate as is the wild-type enzyme, but reduced Asp139Asn is unreactive with thioredoxin (S. B. Mulrooney and C. H. Williams, Jr, personal communication).

The substrate for thioredoxin reductase is oxidized *Escherichia coli* thioredoxin, the structure of which has been determined at 1·68 Å resolution by X-ray crystallography (Katti *et al.*, 1990). In its oxidized configuration, the disulfide bond of thioredoxin reductase is not accessible for interaction with the redox active disulfide bond of thioredoxin. Simple modeling studies using the structures of the two proteins make it clear that the formation of a mixed disulfide bond between the two proteins, which is thought to occur during catalysis, would require significant changes in one or both partners. In addition, the isoalloxazine ring system of the FAD is also inaccessible to solvent, making a direct interaction between thioredoxin and the flavin highly unlikely.

4. Discussion

The structure of thioredoxin reductase presents two puzzles. Although the disulfide bond is located close to the flavin ring system, consistent with biochemical experiments, the substrate thioredoxin is too bulky to fit into the space near the disulfide. Also, it is known that the nicotinamide ring of NADPH transfers a hydride ion to the flavin with the same stereospecificity as seen in glutathione reductase (Manstein *et al.*, 1988). That is, at some point in the enzyme reaction, the NADPH group is likely to adopt a conformation similar to that seen in glutathione reductase and excluded in this structure of thioredoxin reductase by the orientation of the NADPH domain.

Figure 1 illustrates the major differences between the crystal structure of glutathione reductase and that of thioredoxin reductase. While the topology of the active site in glutathione reductase explains the flow of electrons from NADPH to glutathione, it is difficult to envisage a similar mechanism in thioredoxin reductase (Shultz, 1992). This discrepancy is a direct consequence of the position of the redox active cysteine pair in the amino acid sequence of thioredoxin reductase with the redox active disulfide located in the pyridine nucleotide domain rather than in the FAD domain as in glutathione reductase and lipoamide dehydrogenase (Russel & Model, 1988). The structures reported here confirm that the different compartments of the active site in thioredoxin reductase have undergone a profound reorganization, with no close contact (in this conformation of the enzyme) between the nicotinamide ring of the NADPH and the isoalloxazine ring system of the FAD, and with the redox active disulfide interposing between the two dinucleotides. However, extensive similarities between individual FAD and NADPH domains of both glutathione reductase and thioredoxin reductase hint at a possible reaction mechanism.

As mentioned above, the NADPH domains of thioredoxin reductase and glutathione reductase are very similar. If the FAD domains are first aligned, the NADPH domains can be superimposed by rotating one of them by 66°. When such a rotation is applied to the NADPH domain of thioredoxin reductase, leaving its FAD domain fixed, the nicotinamide ring of NADPH is brought in close contact to the isoalloxazine ring system with the nicotinamide C-4 above the isoalloxazine N-5 (Fig. 13). These two atoms are responsible for

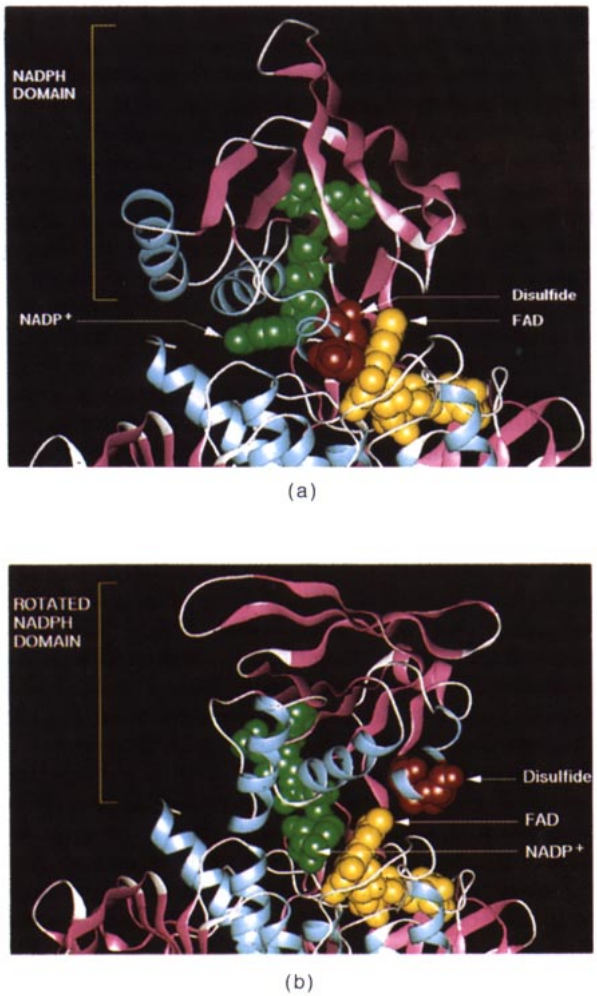

Figure 13. The proposed conformational change. The conformational change involves a 66° rotation of the NADPH domain about the 2 strands connecting this domain and the FAD domain. This results in a conformation that resembles glutathione reductase in terms of the relative orientation of the NADPH and FAD domains. Schematic drawings of thioredoxin reductase are shown before (a) and after (b) the conformational change. α-Helices are shown in light blue, β-strands in pink, and non-regular structure in white. $NADP^+$, FAD and the redox active disulphide are shown as solid spheres with $NADP^+$ in green, FAD in yellow, and the redox active disulphide in red.

hydride transfer between the two dinucleotides (Blackenhorn, 1976). This juxtapositioning is a consequence of the fact that this rotation of the NADPH domain in thioredoxin reductase results in a conformation that mimics that of glutathione reductase.

When this rotation is applied, the redox active dithiol moves to the surface of the protein where it is now accessible to thioredoxin. It is important to note that there is no large steric hindrance to prevent this rotation from happening in thioredoxin reductase. We modeled 5 degree rotation steps around the rotation axis and showed that the NADPH domain can rotate around this axis without severe close contacts being created. Optimization of the modeled structure by energy minimization resulted in a structure with no close contacts that cannot be alleviated by repositioning side-chains (which we have not attempted). Interestingly, the rotated glutathione reductase-like configuration allows a cluster of charged residues (Arg181, Glu183, Lys184) to fit into a charged pocket formed on the other monomer by the tip of the C-terminal helix and the loop connecting residue 24 to residue 29. This dimer interface interaction could stabilize the NADPH domain onto the FAD domain in its rotated conformation.

There is as yet no conclusive biochemical evidence for the proposed mechanism. In thioredoxin reductase, both thiols at the active site are reactive to alkylation, which had been interpreted as evidence for a more open active site in this enzyme than in glutathione reductase or lipoamide dehydrogenase, where only the thiol that interacts with substrate can be alkylated (Thorpe & Williams, 1976; Arscott *et al.*, 1981). The crystal structures of thioredoxin reductase that we have determined show, however, that only one thiol (Cys135) is accessible to solvent (based on surface calculations using a probe of radius 1·4 Å (Richards, 1977)). Thus, the bis-alkylation of reduced thioredoxin reductase may result from the rotation proposed here rather than a more open active site. Altered forms of the enzyme in which the active center cysteine residues have been singly changed to serine (Cys135Ser) and (Cys138Ser) have significant catalytic activity (11% in the case of Cys135Ser). A change in kinetic mechanism made estimation of the catalytic activity of Cys138Ser difficult, but the maximal activity may have been as high as 60% (Prongay *et al.*, 1989). It was suggested that the single remaining thiol could form a mixed disulfide with thioredoxin and that the mixed disulfide could be reduced by $FADH_2$ (Prongay *et al.*, 1989). In the proposed rotated conformation, the mixed disulfide is formed at some distance from the flavin, and it is not clear how this reduction would proceed. Further biochemical experiments, study of the interactions of the crystals with NADPH under anaerobic conditions and additional efforts to stabilize the rotated conformer will be needed to resolve this.

Proteins can undergo major conformational changes upon binding of their substrate. For instance, the binding of glucose triggers a large rearrangement of the two lobes of hexokinase A (McDonald *et al.*, 1979; Bennett & Steitz, 1980). Similar observations have been made with other kinases like adenylate kinase (Schulz *et al.*, 1990). Kinases have to shield their catalytic centers from water to avoid the futile hydrolysis of ATP. For this purpose, kinases undergo an induced-fit movement (Koshland, 1958), the result of which is the protection of the substrate and the active site from water. In oxido-reductases, protection against water is also necessary and, in glutathione reductase, such protection is the result of the packing of the three elements of the active site (the nicotinamide ring,

the isoalloxazine ring and the redox active dithiol) and their buried position inside the molecule or at the dimer interface. In thioredoxin reductase, the NADPH binding site is such that accessibility to solvent is high and that a conformational change is necessary to bury the nicotinamide and stack it against the FAD where electron transfer can then occur.

Supported in part by grants from the National Institutes of Health (GM 45547 to J.K. and GM 21444 to C.H.W.). Diffraction data for the (Cys138Ser) mutant were collected at Brookhaven National Laboratory in the Biology Department single-crystal diffraction facility at beamline X12-C in the National Synchrotron Light Source, supported by the United States Department of Energy, Office of Health and Environmental Research, and by the National Science Foundation. We acknowledge help in use of the facility by R.M. Sweet and his staff. We thank Stephen K. Burley, Peter Model and Jim Pflugrath for assistance and advice.

References

Arscott, L. D., Thorpe, C. & Williams, C. H., Jr (1981). Glutathione reductase from yeast—differential reactivity of the nascent thiols in 2-electron reduced enzyme and properties of a monoalkylated derivative. *Biochemistry*, **20**, 1513–1520.

Bennett, W. S. & Steitz, T. A. (1980). Structure of a complex yeast hexokinase A and glucose. *J. Mol. Biol.* **140**, 211–230.

Blackenhorn, G. (1976). Nicotinamide-dependent one-electron and two-electron (flavin) oxidoreduction: thermodynamics, kinetics and mechanism. *Eur. J. Biochem.* **67**, 67–80.

Brant, D. A. & Schimmel, P. R. (1967). Analysis of the skeletal configuration of crystalline hen egg-white lysozyme. *Proc. Nat. Acad. Sci., U.S.A.* **58**, 428–435.

Brünger, A. T. (1988). X-PLOR (version 2.2) manual. Howard Hughes Medical Institute and Department of Molecular Biophysics and Biochemistry, Yale University, New Haven, CT.

Hol, W. G. J., van Duijnen, P. T. & Berendsen, H. J. C. (1978). The alpha-helix dipole and the properties of proteins. *Nature (London)*, **273**, 443–446.

Hunter, W. N., Bailey, S., Habash, J., Harrop, S. J., Helliwell, J. R., Aboagye-Kwarteng, T., Smith, K. & Fairlamb, A. H. (1992). Active site of trypanothione reductase, a target for rational drug design. *J. Mol. Biol.* **227**, 322–333.

Janin, J. & Chothia, C. (1990). The structure of protein–protein recognition sites. *J. Biol. Chem.* **265**, 16027–16030.

Jones, T. A. (1985). Interactive computer graphics: FRODO. *Methods Enzymol.* **115**, 157–171.

Jones, T. A., Zou, J. Y. & Cowan, S. W. (1991). Improved methods for building protein models in electron density map and the location of errors in these models. *Acta Crystallogr. sect. A*, **47**, 110–119.

Kabsch, W. & Sander, C. (1983). Dictionary of protein secondary structure: pattern recognition of hydrogen-bonded and geometrical features. *Biopolymers*, **22**, 2577–2637.

Karplus, P. A. & Schulz, G. E. (1987). Refined structure of glutathione reductase at 1·54 Å resolution. *J. Mol. Biol.* **195**, 701–729.

Karplus, P. A. & Schulz, G. E. (1989). Substrate binding and catalysis by glutathione reductase as derived from refined enzyme: substrate crystal structures at 2 Å resolution. *J. Mol. Biol.* **210**, 163–180.

Karplus, P. A., Pai, E. F. & Schulz, G. E. (1989). A crystallographic study of the glutathione binding site of glutathione reductase at 0·3 nm resolution. *Eur. J. Biochem.* **178**, 693–703.

Katti, S. K., LeMaster, D. M. & Eklund, H. (1990). Crystal structure of thioredoxin from *Escherichia coli* at 1·68 Å resolution. *J. Mol. Biol.* **212**, 167–184.

Koshland, D. E., Jr (1958). Application of a theory of enzyme specificity to protein synthesis. *Proc. Nat. Acad. Sci., U.S.A.* **44**, 98–104.

Kraulis, P. J. (1991). MOLSCRIPT: a program to produce both detailed and schematic plots of proteins structures. *J. Appl. Crystallogr.* **24**, 946–950.

Kuriyan, J., Wong, L., Russel, M. & Model, P. (1989). Crystallization and preliminary X-ray characterization of thioredoxin reductase from *Escherishia coli*. *J. Biol. Chem.* **264**, 12752–12753.

Kuriyan, J., Kong, X. P., Krishna, T. S. R., Sweet, R. M., Murgolo, N. J., Field, H., Cerami, A. & Henderson, G. B. (1991*a*). X-ray structure of trypanothione reductase from *Crithidia fasciculata* at 2·4 Å resolution. *Proc. Nat. Acad. Sci., U.S.A.* **88**, 8764–8768.

Kuriyan, J., Krishna, T. S. R., Wong, L., Guenther, B., Pahler, A., Williams, C. H., Jr & Model, P. (1991*b*). Convergent evolution of similar function in two structurally divergent enzymes. *Nature (London)*, **352**, 172–174.

Luzzati, V. (1952). Traitement statistique des erreurs dans la détermination des structures crystallines. *Acta Crystallogr.* **5**, 801–810.

Manstein, D. J., Massey, V., Ghisla, S. & Pai, E. F. (1988). Stereochemistry and accessibility of prosthetic groups in flavoproteins. *Biochemistry*, **27**, 2300–2305.

Mattevi, A., Schierbeek, A. J. & Hol, W. G. J. (1991). The refined crystal structure of lipoamide dehydrogenase from azotobacter vinelandii at 2·2 Å resolution. *J. Mol. Biol.* **220**, 975–994.

Matthews, R. G. & Williams, C. H., Jr (1976). Measurement of the oxidation-reduction potentials for two electron and four electron reduction of lipoamide dehydrogenase from pig heart. *J. Biol. Chem.* **251**, 3956–3964.

McDonald, R. C., Steitz, T. A. & Engelman, D. M. (1979). Yeast hexokinase in solution exhibits a large conformational change upon binding glucose or glucose 6-phosphate. *Biochemistry*, **18**, 338–342.

Moore, E. C., Reichard, P. & Thelander, L. (1964). Enzymatic synthesis of deoxyribonucleotides. V. Purification and properties of thioredoxin reductase from *Escherishia coli B*. *J. Biol. Chem.* **239**, 3445–3452.

O'Donnell, M. E. & Williams, C. H., Jr (1983). Proton stoichiometry in the reduction of the FAD and disulfide of *Escherichia coli* thioredoxin reductase. *J. Biol. Chem.* **258**, 13795–13805.

O'Donnell, M. E. & Williams, C. H., Jr (1985). Reaction of both active site thiols of reduced thioredoxin reductase with N-ethylmaleimide. *Biochemistry*, **24**, 7617–7621.

Pai, E. F. & Schulz, G. E. (1983). The catalytic mechanism of glutathione reductase as derived from X-ray diffraction analyses of reaction intermediates. *J. Biol. Chem.* **258**, 1752–1757.

Pai, E. F., Karplus, A. P. & Schulz, G. E. (1988). Crystallographic analysis of the binding of NADPH,

NADPH fragments, and NADPH analogues to glutathione reductase. *Biochemistry*, **27**, 4465–4474.

Peters, D. & Peters, J. (1981). Quantum theory of the structure and bonding in proteins. *J. Mol. Struct.* **85**, 107–123.

Prongay, A. J. & Williams, C. H., Jr (1990). Evidence for direct interaction between cysteine 138 and the flavin in thioredoxin reductase. A study using flavin analogs. *J. Biol. Chem.* **265**, 18968–18975.

Prongay, A. J. & Williams, C. H., Jr (1992). Oxidation-reduction properties of *Escherichia coli* thioredoxin reductase altered at each active site cysteine residues. *J. Biol. Chem.* **266**, 25181–25188.

Prongay, A. J., Engelke, D. R. & Williams, C. H., Jr (1989). Characterization of two active site mutants of thioredoxin reductase from *Escherishia coli*. *J. Biol. Chem.* **264**, 2656–2664.

Ramachandran, G. N. & Sasisekharan, V. (1968). Conformations of polypeptides and proteins. *Advan. Protein Chem.* **23**, 283–437.

Richards, F. M. (1977). Areas, volumes, packing and protein structure. *Annu. Rev. Biophys. Bioeng.* **6**, 151–176.

Ronchi, S. & Williams, C. H., Jr (1967). The isolation and primary structure of a peptide containing the oxidation-reduction active cysteine of *Escherichia coli* thioredoxin reductase. *J. Biol. Chem.* **247**, 2083–2086.

Rossmann, M. G., Liljas, A., Bränden, C. I. & Benaszak, L. J. (1975). Evolutionary and structural relationships among dehydrogenases. In *The Enzymes* (Boyer, P. D., ed.), vol. 11, pp. 61–102, Academic Press, New York.

Russel, M. & Model, P. (1988). Sequence of thioredoxin reductase from *Escherishia coli*. *J. Biol. Chem.* **263**, 9015–9019.

Schiering, N., Kabsch, W., Moore, M. J., Distefano, M. D., Walsh, C. T. & Pai, E. F. (1991). Structure of the detoxification catalyst mercuric ion reductase from *Bacillus sp.* strain RC607. *Nature (London)*, **352**, 168–172.

Schirmer, R. H. & Schulz, G. E. (1987). Pyridine nucleotide-linked sulfur metabolism. In *Coenzymes and Cofactors, Pyridine Nucleotide Coenzymes: Chemical, Biochemical and Medical Aspects* (Dalphin, D., Poulson, R. & Avramovic, O., eds), pp. 333–379, Wiley, New York.

Schulz, G. E. (1980). Gene duplication in glutathione reductase. *J. Mol. Biol.* **138**, 335–347.

Schulz, G. E. (1992). Binding of nucleotides by proteins. *Curr. Opin. in Struc. Biol.* **2**, 61–67.

Schulz, G. E., Schirmer, R. H., Sachsenheimer, W. & Pai, E. F. (1978). The structure of the flavoenzyme glutathione reductase. *Nature (London)*, **273**, 120–124.

Schulz, G. E., Schirmer, R. H. & Pai, E. F. (1982). FAD-binding site of glutathione reductase. *J. Mol. Biol.* **160**, 287–308.

Schulz, G. E., Müller, C. W. & Diederichs, K. (1990). Induced-fit movements in adenylate kinases. *J. Mol. Biol.* **213**, 627–630.

Stehle, T., Ahmed, S. A., Claiborne, A. & Schulz, G. E. (1991). Structure of NADH peroxidase from *Streptococcus faecalis* 10C1 refined at 2·16 Å resolution. *J. Mol. Biol.* **221**, 1325–1344.

Stehle, T., Claiborne, A. & Schulz, G. E. (1993). NADH binding site and catalysis of NADH peroxidase. *Eur. J. Biochem.* **211**, 221–226.

Thelander, L. (1968). Studies on thioredoxin reductase from *Escherishia coli* B. The relation of structure and function. *Eur. J. Biochem.* **4**, 407–422.

Thieme, R., Pai, E. F., Schirmer, R. H. & Schulz, G. E. (1981). Three-dimensional structure of glutathione reductase at 2 Å resolution. *J. Mol. Biol.* **152**, 763–782.

Thorpe, C. & Williams C. H., Jr (1976). Spectral evidence for a flavin adduct in a monoalkylated derivative of pig heart lipoamide dehydrogenase. *J. Biol. Chem.* **251**, 7726–7728.

Weis, W. I., Brünger, A. T., Skehel, J. J. & Wiley, D. C. (1990). Refinement of the influenza virus hemagglutinin by simulated annealing. *J. Mol. Biol.* **212**, 737–761.

Wierenga, R. K., de Jong, R. J., Kalk, K. H., Hol, W. G. J. & Drenth, J. (1979). Crystal structure of *p*-hydroxybenzoate hydroxylase. *J. Mol. Biol.* **131**, 55–73.

Wierenga, R. K., Drenth, J. & Schulz, G. E. (1983). Comparison of the three-dimensional protein and nucleotide structure of the FAD-binding domain of *p*-hydroxybenzoate hydroxylase with the FAD- as well as the NADPH-binding domains of glutathione reductase. *J. Mol. Biol.* **167**, 725–739.

Williams, C. H., Jr (1992). Lipoamide dehydrogenase, glutathione reductase, thioredoxin reductase, and mercuric ion reductase—A family of flavoenzyme transhydrogenase. In *Chemistry and Biochemistry of Flavoenzymes* (Müller, F., ed.), vol 3, pp. 121–211, CRC Press, Inc, Boca Raton, FL.

Williams, C. H., Jr, Prongay, A. J., Lennon, B. W. & Kuriyan, J. (1991). Pyridine nucleotide-disulfide oxidoreductases—overview of the family and some properties of thioredoxin reductase altered by site directed mutagenesis: C135S and C138S. In *Flavins and Flavoproteins* (Curti, B., Zannetti, G. & Ronchi, S., eds), pp 497–504, Walter de Gruyter and Co., Berlin.

Wong, D. J., Vanoni, M. A. & Blanchard, J. S. (1988). Glutathione reductase: solvent equilibrium and kinetic isotope effects. *Biochemistry*, **27**, 7091–7096.

Zanetti, G. & Williams, C. H., Jr (1967). Characterization of the active center of thioredoxin reductase. *J. Biol. Chem.* **242**, 5232–5236.

Edited by I. A. Wilson

(Received 30 June 1993; accepted 4 November 1993)